Electronic Supplementary Material (ESI) for Photochemical & Photobiological Sciences.
This journal is © The Royal Society of Chemistry and Owner Societies 2019

Supporting Information

Core-shell polymeric nanoparticles comprising BODIPY and fluorescein as ultra-bright ratiometric fluorescent pH sensors

C. Grazon,*[a]† Y. Si,[a] J.-P. Placial,[a] J. Rieger,[b] R. Méallet-Renault[a,]§ and G. Clavier[a]

[a] PPSM, ENS Cachan, CNRS, Université Paris-Saclay, 94235 Cachan, France

E-mail: chloe.grazon@u-bordeaux.fr

[b] Sorbonne Université, CNRS, Institut Parisien de Chimie Moléculaire, UMR 8232, Team : Chimie des Polymères, 75005 Paris, France.

Current addresses:

† Laboratoire de Chimie des Polymères Organiques (LCPO), CNRS UMR 5629, Université de Bordeaux, Bordeaux-INP, Pessac 33607 Cedex, France.

§ Institut des Sciences Moléculaires d'Orsay (ISMO), CNRS, Univ. Paris-Sud, Université Paris-Saclay, F-91405 Orsay (France).

Equations

The aggregation number N_{agg} was calculated using the equation:

$$N_{agg} = \frac{n_{chain}}{n_{FNP}} = \frac{V_{FNP}}{V_S} \times n_{chain} = \frac{\frac{4}{3}\pi r^3}{m_S \rho_S} \times n_{chain} \quad \text{(S1)}$$

where n_{chain} is the total number of growing chains (which is equal to the number of macroRAFT agent assuming they are all incorporated in the nanoparticles), n_{FNP} is the number of fluorescent nanoparticles, V_S the total volume of styrene in the synthesis, V_{FNP} is the volume of one fluorescent nanoparticle, m_S the total mass of styrene in the synthesis, ρ_S the polystyrene density and r the core radius of the nanoparticles determined by TEM microscopy (Figure S1).

The number of BODIPY monomer (η_{BOD}) per polymer chain was calculated using the equation:

$$\eta_{BOD} = \frac{n_{BOD}}{n_{RAFT}} \quad \text{(S2)}$$

where n_{BOD} and n_{RAFT} are respectively the moles number of BOD and macroRAFT agent used in the nanoparticles synthesis.

The number of BODIPY monomer (N_{BOD}) per FNP was calculated using the equation:

$$N_{BOD} = N_{agg} \times \eta_{BOD} \quad \text{(S3)}$$

The brightness (B) of the FNP containing only one type of dye was calculated using the equation:

$$B = \varepsilon_\lambda \times N \times \Phi_F \quad \text{(S4)}$$

Where ε_λ is the molar absorption coefficient of the dye at the wavelength (λ) of excitation, Φ_F the fluorescent quantum yield of the nanoparticles and N the number of dyes per nanoparticle.

Synthesis of FNP

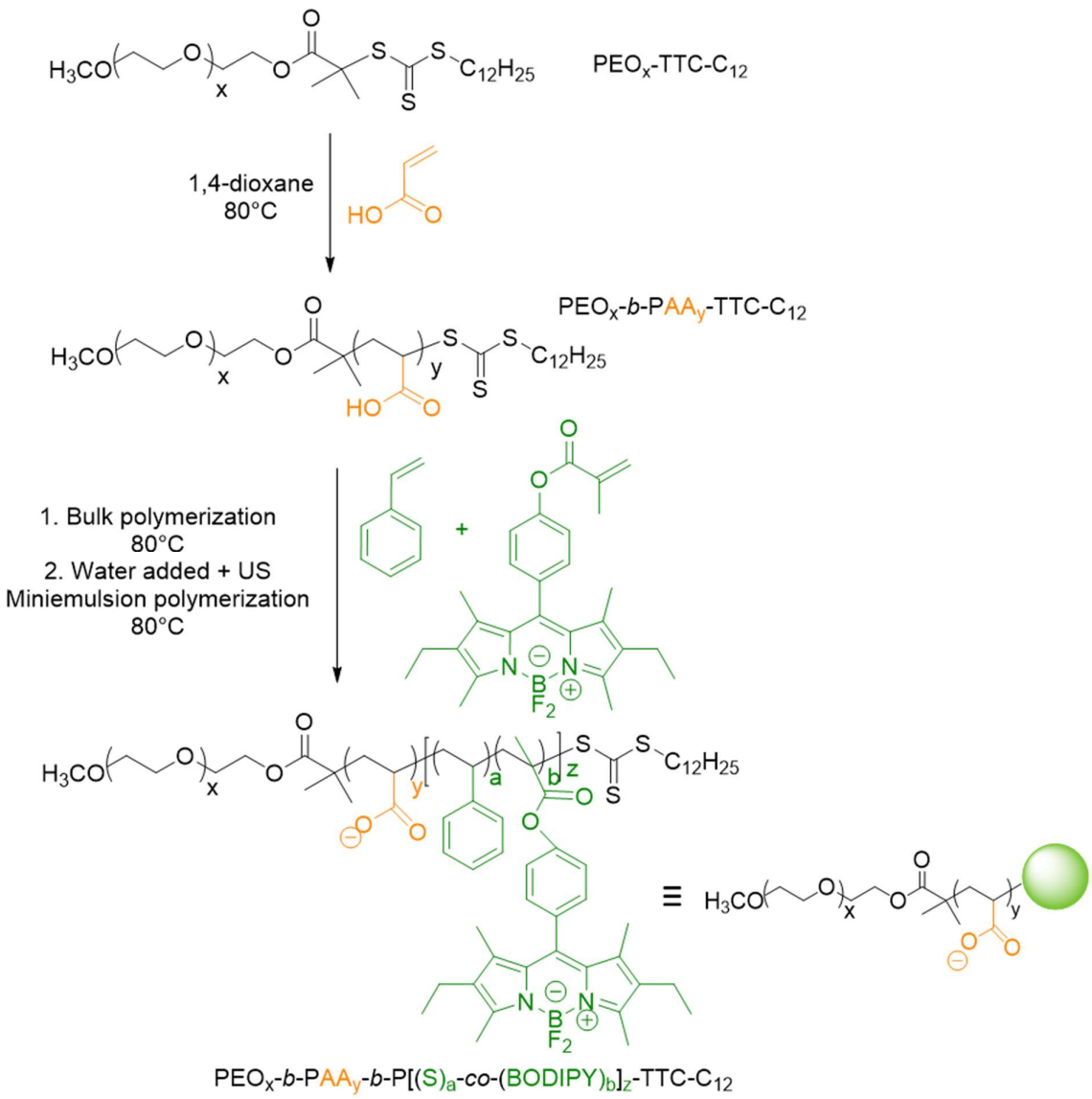

Scheme S1. Synthetic scheme employed for the synthesis of the fluorescent nanoparticles **FNP1$_{BOD}$** stabilized by a double hydrophilic block copolymer (PEO-*b*-PAA shell).

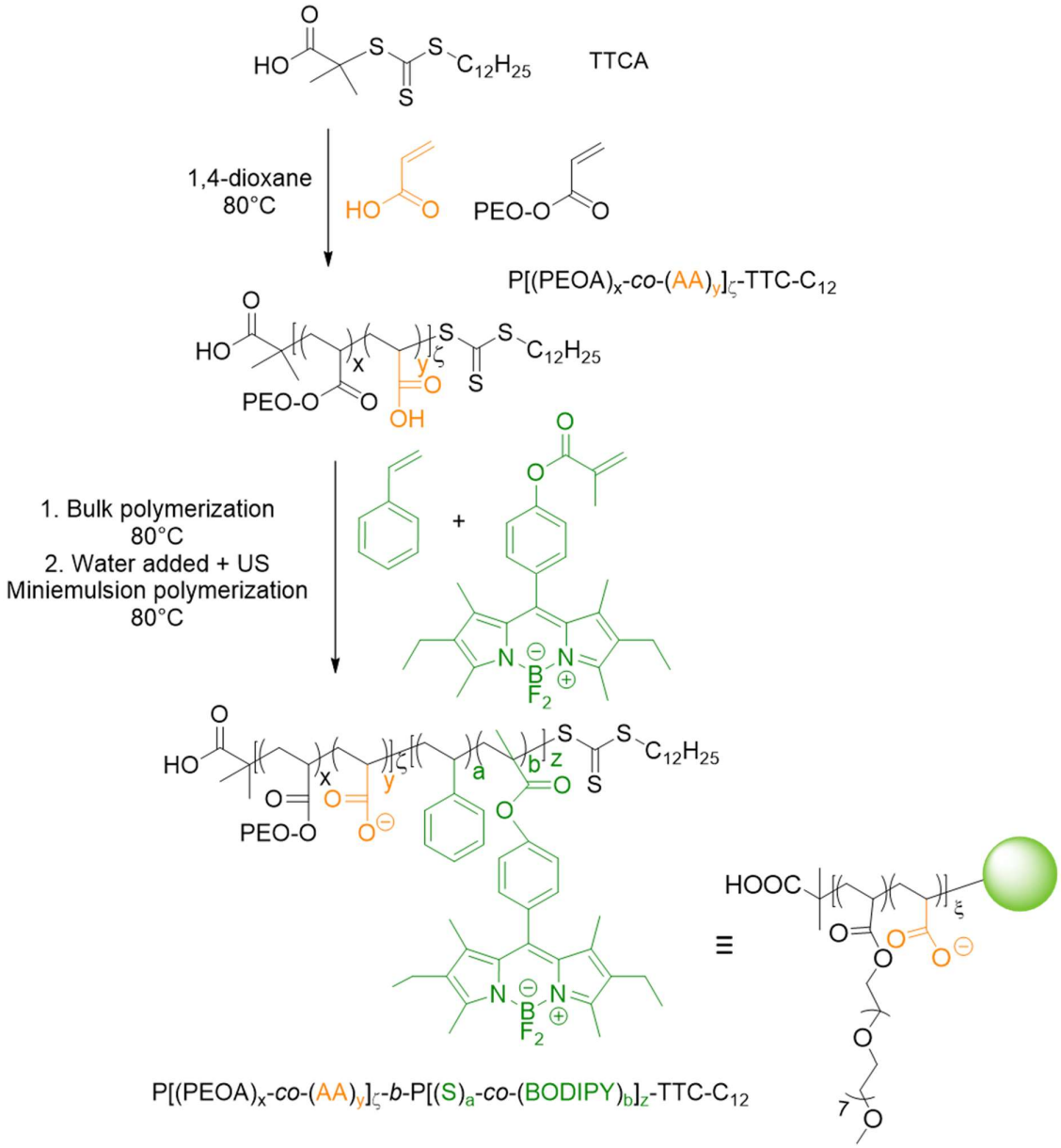

Scheme S2. Synthetic scheme employed for the synthesis of the fluorescent nanoparticles **FNP2$_{BOD}$** stabilized by a hydrophilic random copolymer (P[(PEOA)-*co*-(AA)] shell).

Table S1. Characterization of fluorescent nanoparticles (FNP) having different shells, synthesized *via* a one-pot miniemulsion polymerization.

Sample	shell	n_{BOD}[a]	conv.$_S$[b]	conv.$_{BOD}$[c]	$M_{n,th}$ [kg/mol] [d]	$M_{n,SEC}$ [kg/mol] [e]	M_w/M_n[e]	D_h (σ)[f] nm
FNP1$_{BOD}$	PEO_{45}-*b*-PAA_{15}	1.1	0.91	0.99	15.2	23.7	1.45	76 (0.12)
FNP1	PEO_{45}-*b*-PAA_{19}	0	0.97	-	14.2	16.8	1.29	80 (-)
FNP2$_{BOD}$	$P(AA_{0.5}$-*co*-$PEOA_{0.5})_{22}$	2.0	0.97	0.97	22.4	18.5	1.40	77 (0.10)
FNP2	$P(AA_{0.5}$-*co*-$PEOA_{0.5})_{22}$	0	0.85	-	19.7	17.1	1.35	70 (0.12)

[a] Average number of BODIPY per polymer chain (with a $DP_{n,total}$ about 120), calculated using eq. S2. [b] Styrene conversion determined by gravimetry. [c] BODIPY conversion determined by SEC by comparison of the calculated area of the polymer and monomer peaks from SEC equipped with a UV-vis detector (C. Grazon, *et al*. *Macromol. Rapid Commun.* 2011, **32**, 699). [d] Theoretical number-average molar mass ($M_{n\ th} = M_{n\ CTA} + 1/n_{CTA}\times(conv._S\times m_S+conv._{BOD}\times m_{BOD})$, where CTA stands for chain transfer agent, conv.$_S$ and conv.$_{BOD}$ the individual conversion of styrene and BODIPY and m the mass of monomer used in the synthesis). [e] Number-average molar mass ($M_{n,SEC}$) and molar mass dispersity (M_w/M_n) determined by SEC using a polystyrene calibration. [f] Hydrodynamic diameter (D_h) and dispersity factor (σ) determined by DLS.

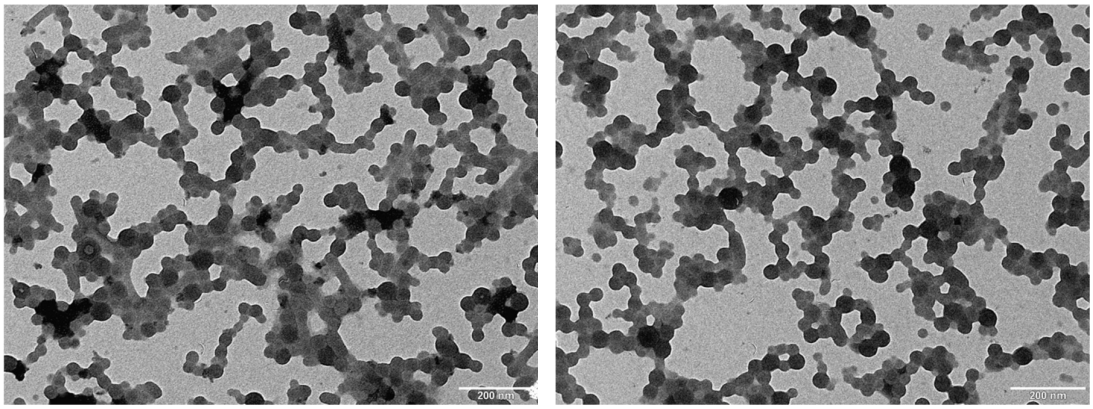

Figure S1. Transmission electron microscopy photographs of the dried fluorescent nanoparticles (scale bar: 200 nm). Left: **FNP1$_{BOD-FA}$** and right: **FNP2$_{BOD-FA}$**.

Spectroscopic characterizations of FNP_{BOD}

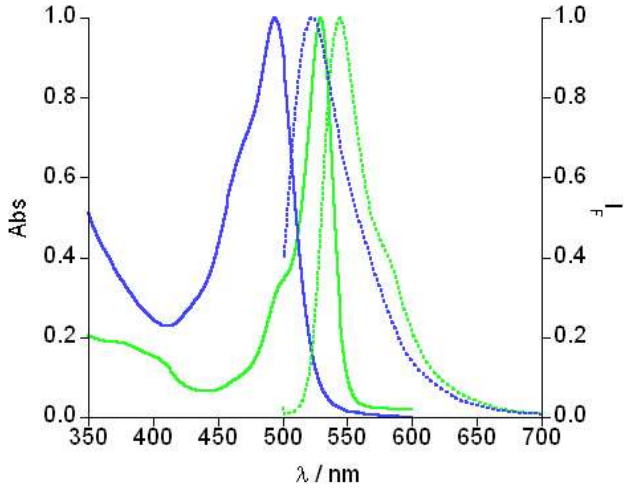

Figure S2. Normalized absorption (full lines) and fluorescence emission spectra (dotted lines, λ_{exc} = 495 nm) of **$FNP1_{BOD}$** (▬) and **$FNP1_{FA}$** (▬) at pH = 8.

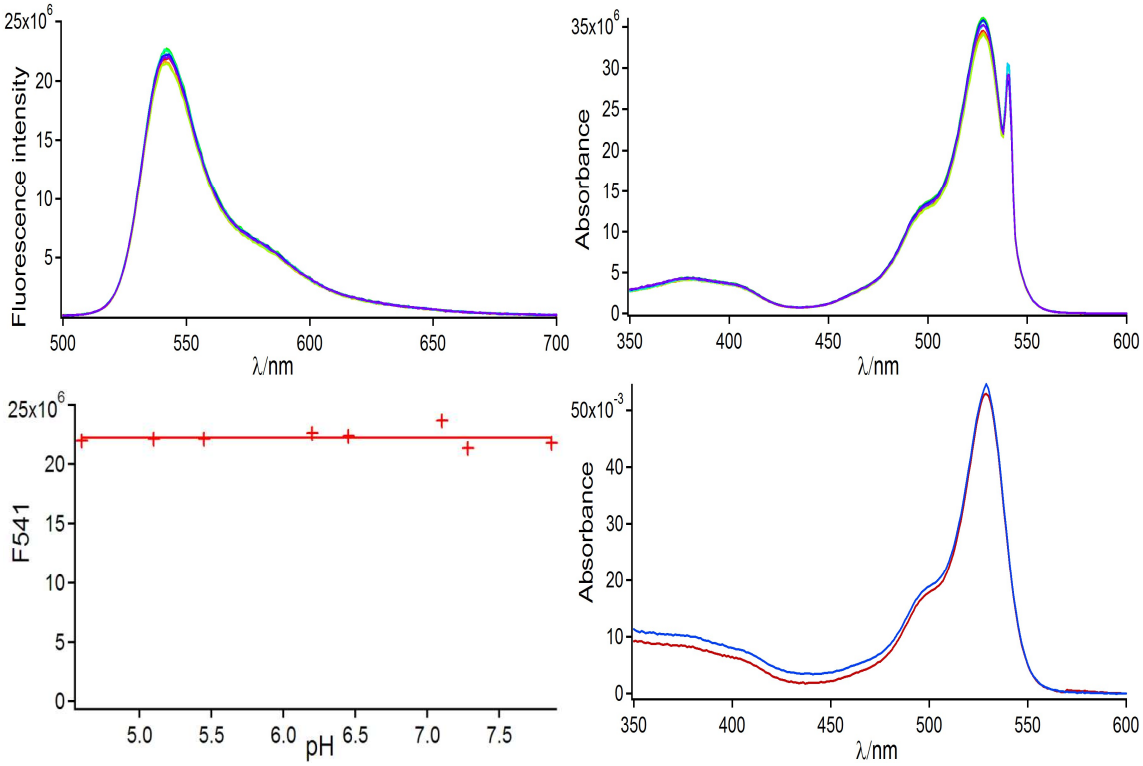

Figure S3. Top left: fluorescence emission spectra of **$FNP1_{BOD}$** at various pH (λ_{ex}=495nm); Top right: fluorescence excitation spectra of **$FNP1_{BOD}$** at various pH (λ_{em}=550nm). Bottom: variation of fluorescence intensity at 541nm as a function of the pH (+) and fit using a straight line. Conditions: phosphate/citrate buffers 1mM in 140mM NaCl; pH values: 7.86, 7.28, 7.10, 7.00, 6.45, 6.20, 5.45, 5.10, 4.60. Bottom right: absorption spectra (pH=4: red line, pH=8: blue line).

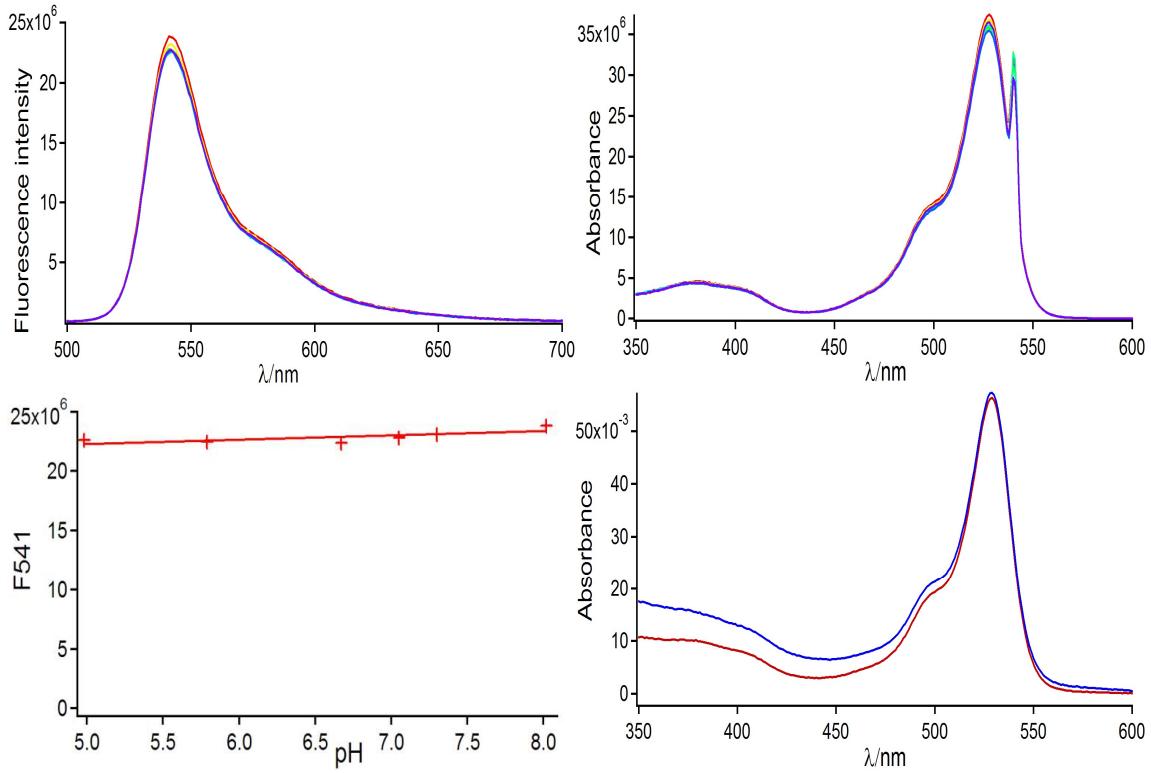

Figure S4. Top left: fluorescence emission spectra of **FNP1$_{BOD}$** at various pH (λ_{ex}=495nm); Top right: fluorescence excitation spectra of **FNP1$_{BOD}$** at various pH (λ_{em}=550nm). Bottom: variation of fluorescence intensity at 541nm as a function of the pH (+) and fit using a straight line. Conditions: phosphate/citrate buffers 10mM in 140mM NaCl; pH values: 8.02, 7.30, 7.05, 6.67, 5.79, 4.98. Bottom right: absorption spectra (pH=4: red line, pH=8: blue line).

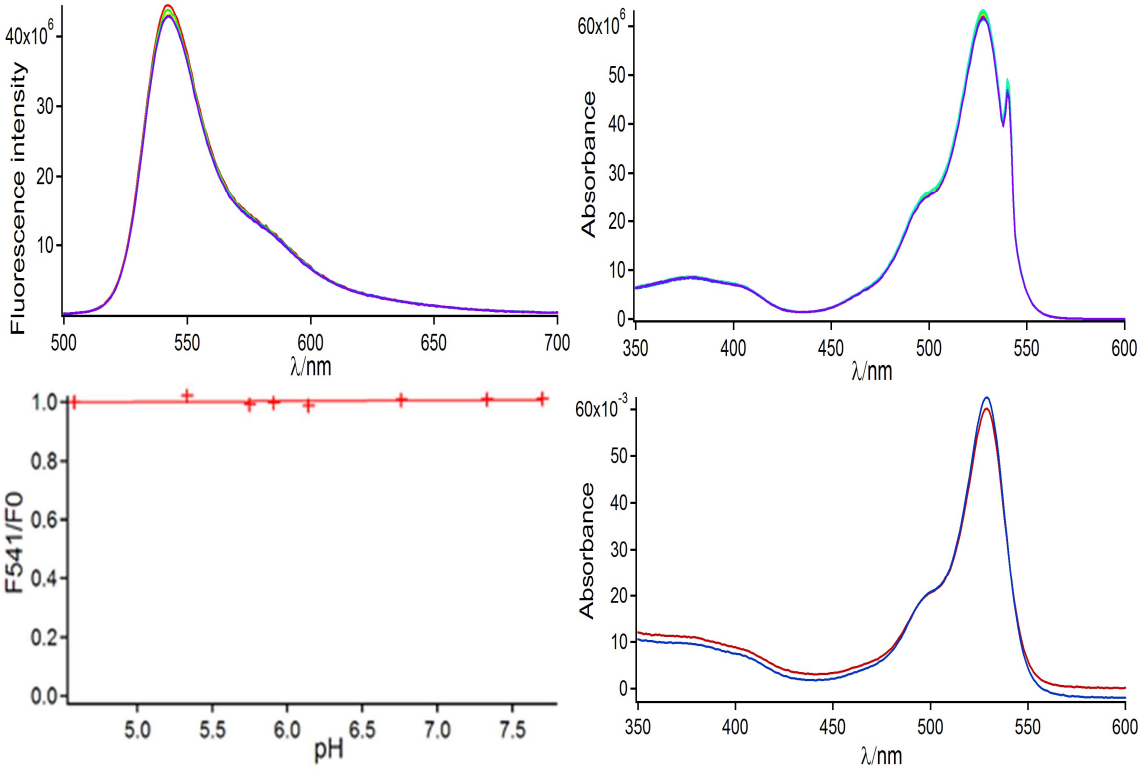

Figure S5. Top left: fluorescence emission spectra of **FNP2$_{BOD}$** at various pH (λ_{ex}=495nm); Top right: fluorescence excitation spectra of **FNP2$_{BOD}$** at various pH (λ_{em}=550nm). Bottom left: relative variation of fluorescence intensity at 541nm as a function of the pH (+) and fit using a straight line (F0: fluorescence intensity at 541nm when pH=4.58). Conditions: phosphate/citrate buffers 1mM in 140mM NaCl; pH values: 4.58, 5.33, 5.75, 5.91, 6.14, 6.76, 7.33 and 7.70. Bottom right: absorption spectra (pH=4: red line, pH=8: blue line).

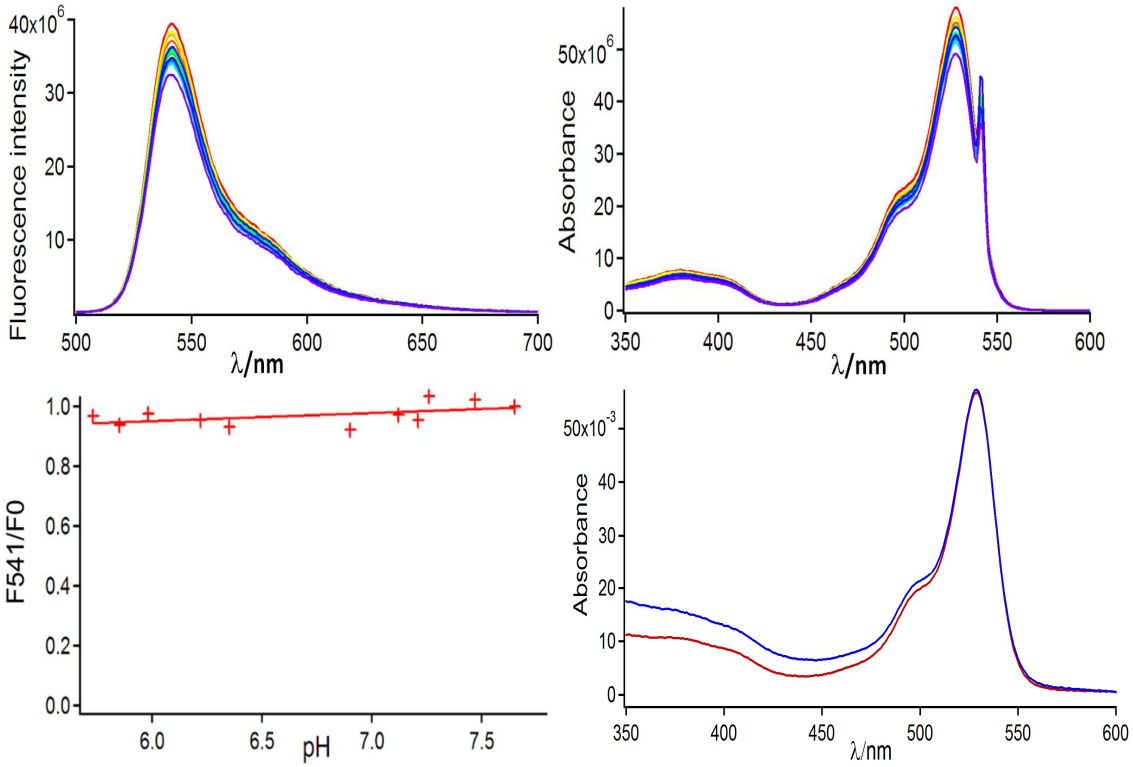

Figure S6. Top left: fluorescence emission spectra of **FNP2$_{BOD}$** at various pH (λ_{ex}=495nm); Top right: fluorescence excitation spectra of **FNP2$_{BOD}$** at various pH (λ_{em}=550nm). Bottom: relative variation of fluorescence intensity at 541nm as a function of the pH (+) and fit using a straight line (F0: fluorescence intensity at 541nm when pH=7.65). Conditions: phosphate/citrate buffers 10mM in 140mM NaCl; pH values: 7.65, 7.47, 7.26, 7.21, 7.12, 6.90, 6.35, 6.22, 5.98, 5.85, 5.73, 5.36. Bottom right: absorption spectra (pH=4: red line, pH=8: blue line).

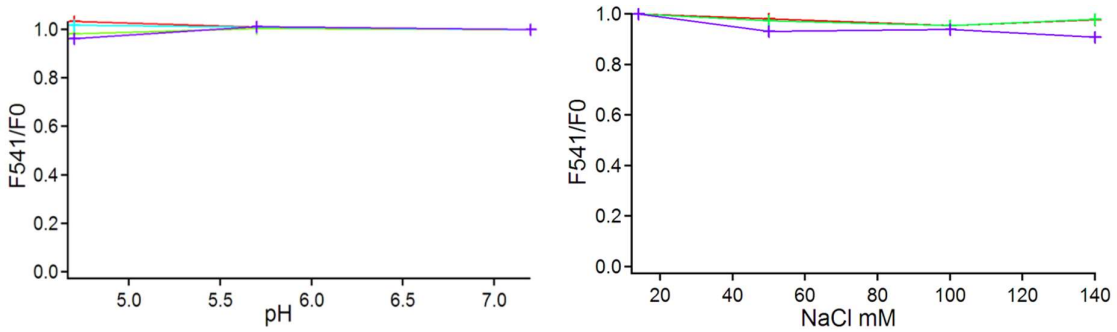

Figure S7. Left: relative variation of fluorescence intensity of **FNP1$_{BOD}$** at 541nm as a function of the pH in 1mM phosphate/citrate buffers and at various NaCl concentrations: 14 mM (red), 50 mM (green), 100 mM (blue) and 140 mM (purple); pH values: 4.7, 5.7 and 7.2. (F0: fluorescence intensity of **FNP1$_{BOD}$** at 541nm when pH=7.2). Right: relative variation of fluorescence intensity of **FNP1$_{BOD}$** at 541nm as a function of NaCl concentration in phosphate/citrate buffers 1mM and at various pH values: 4.7 (purple), 5.7 (green) and 7.2 (red); NaCl concentrations: 14mM, 50mM, 100mM and 140mM. (F0: fluorescence intensity of **FNP1$_{BOD}$** at 541nm when NaCl concentration= 14mM).

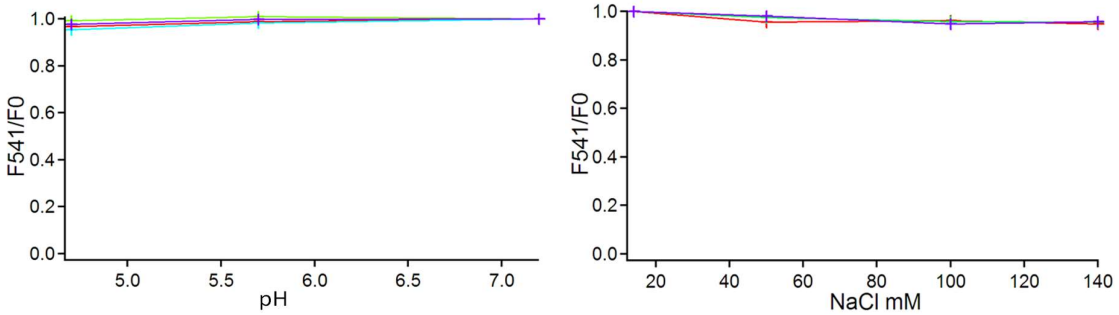

Figure S8. Left: relative variation of fluorescence intensity of **FNP2$_{BOD}$** at 541nm as a function of the pH in 1mM phosphate/citrate buffers and at various NaCl concentrations: 14 mM (red), 50 mM (green), 100 mM (blue) and 140 mM (purple) and fit using a straight line. pH values: 4.7, 5.7 and 7.2. (F0: fluorescence intensity of **FNP2$_{BOD}$** at 541nm when pH=7.2). Right: relative variation of fluorescence intensity of **FNP2$_{BOD}$** at 541nm as a function of NaCl concentration in 1mM phosphate/citrate buffers at various pH values: 4.7 (purple), 5.7 (green) and 7.2 (red); NaCl concentrations: 14mM, 50mM, 100mM and 140mM. (F0: fluorescence intensity of **FNP2$_{BOD}$** at 541nm when NaCl concentration= 14mM).

Spectroscopic characterizations of FNP_{FA}

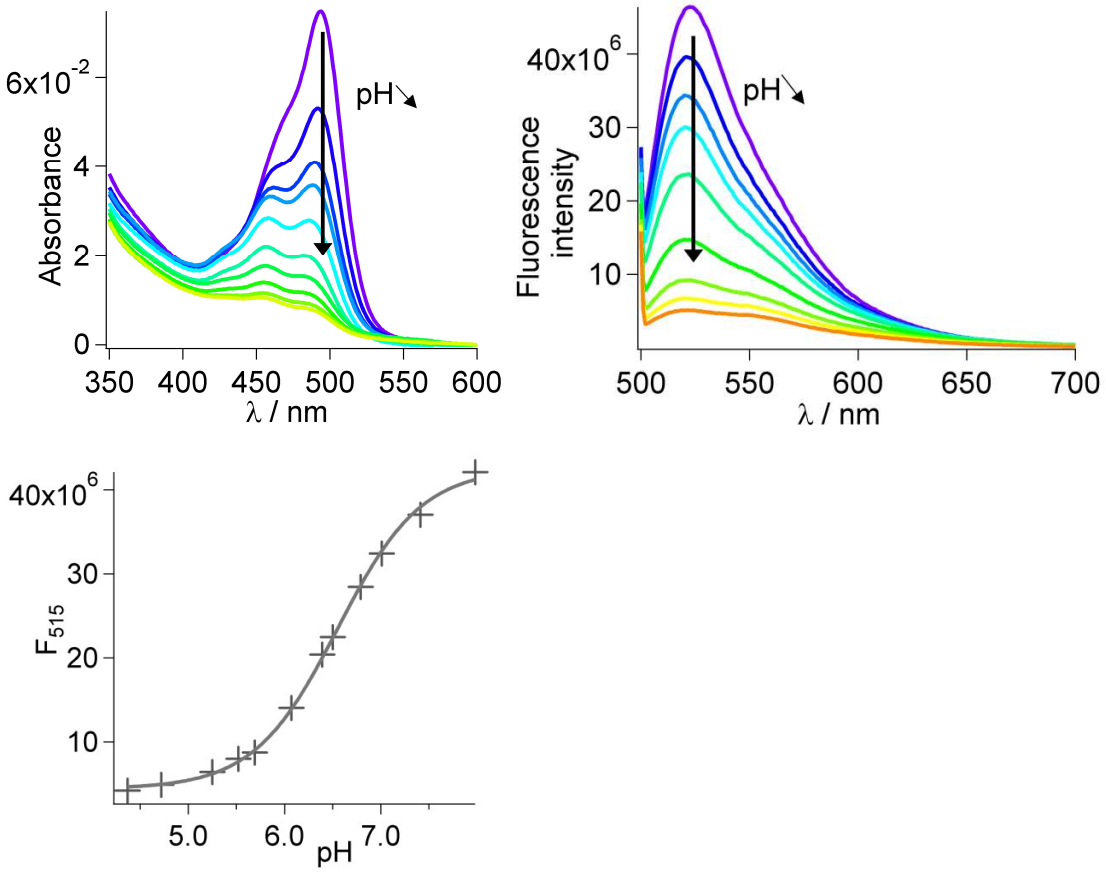

Figure S9. Top left: absorption spectra of **$FNP1_{FA}$** at various pH. Top right: fluorescence emission spectra of **$FNP1_{FA}$** at various pH (λ_{exc} = 495 nm). Bottom: variation of fluorescence intensity at 515 nm as a function of the pH (+) and fit using the Henderson-Hasselbach equation 2 with pKa = 6.55 (—). pH values: 7.98, 7.41, 7.01, 6.79, 6.50, 6.39, 6.07, 5.69, 5.52, 5.25, 4.72, 4.37.

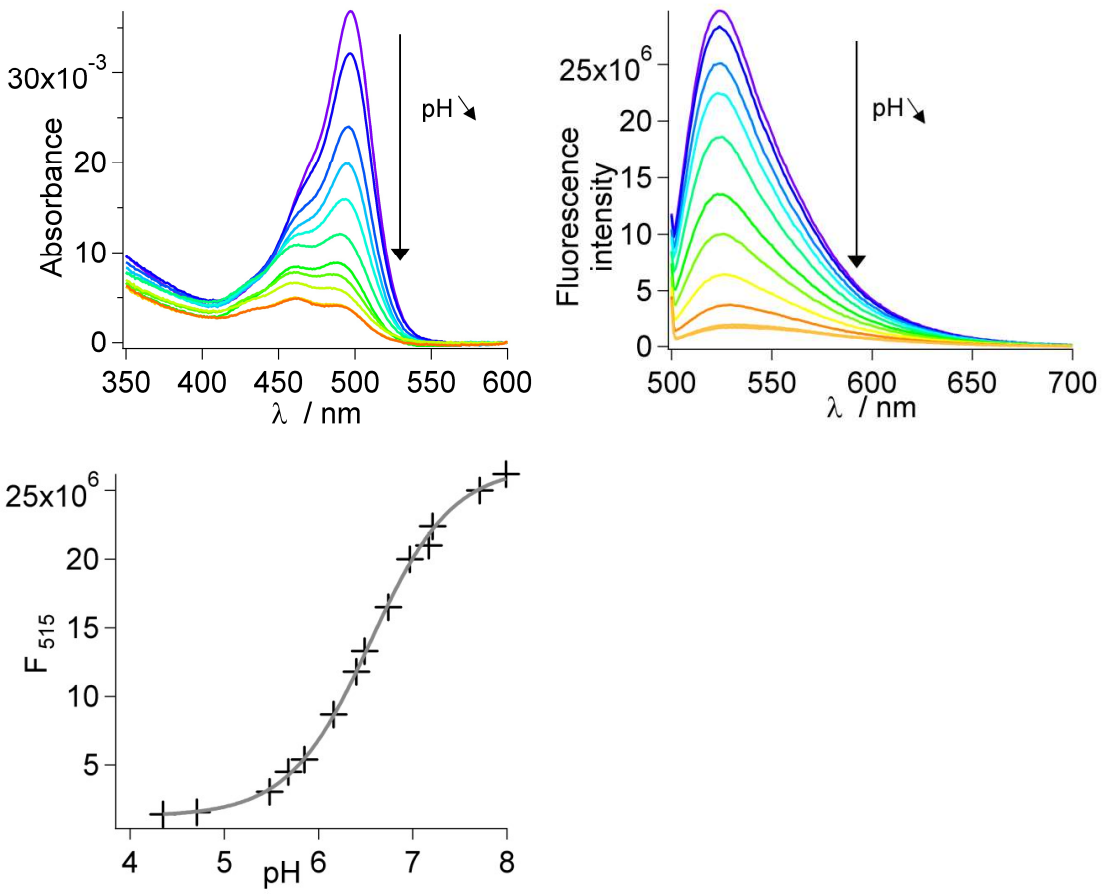

Figure S10. Top left: absorption spectra of **FNP2$_{FA}$** at various pH. Top right: fluorescence emission spectra of **FNP2$_{FA}$** at various pH (λ_{exc} = 495 nm). Bottom: variation of fluorescence intensity at 515 nm as a function of the pH (+) and fit using the Henderson-Hasselbach equation 2 with pKa = 6.55 (—). pH values: 7.99, 7.71, 7.21, 7.17, 6.97, 6.74, 6.49, 6.40, 6.16, 5.85, 5.68, 5.48, 4.71, 4.35.

Absorption and emission spectra of $FNP_{BOD\text{-}FA}$ with pH

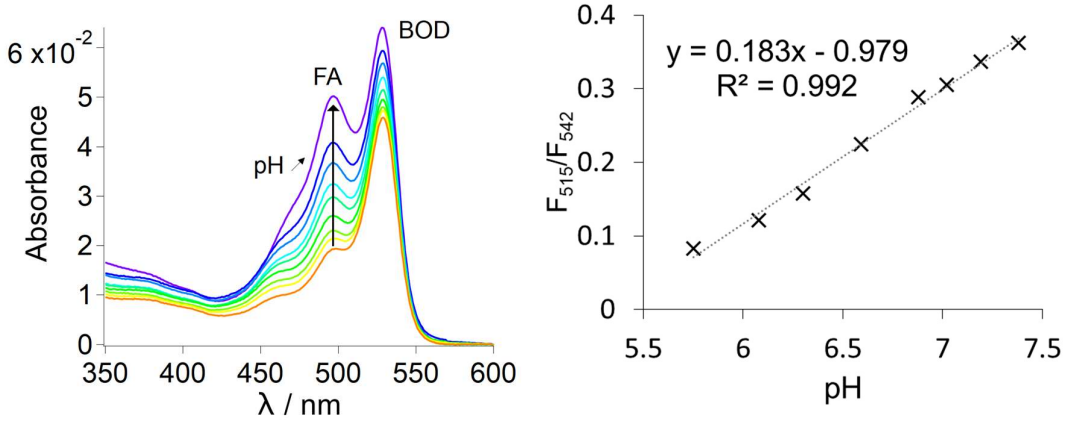

Figure S11. Left: absorption spectra of **$FNP1_{BOD\text{-}FA}$** at various pH (phosphate/citrate buffers 10mM in 140mM NaCl; pH values: 8.01, 7.38, 7.19, 7.02, 6.88, 6.59, 6.30, 6.08, 5.75). Right: variation of the ratio of fluorescence intensity at 515 and 542 nm as a function of the pH (between pH = 5.5 and 7.5) and fit using a linear equation.

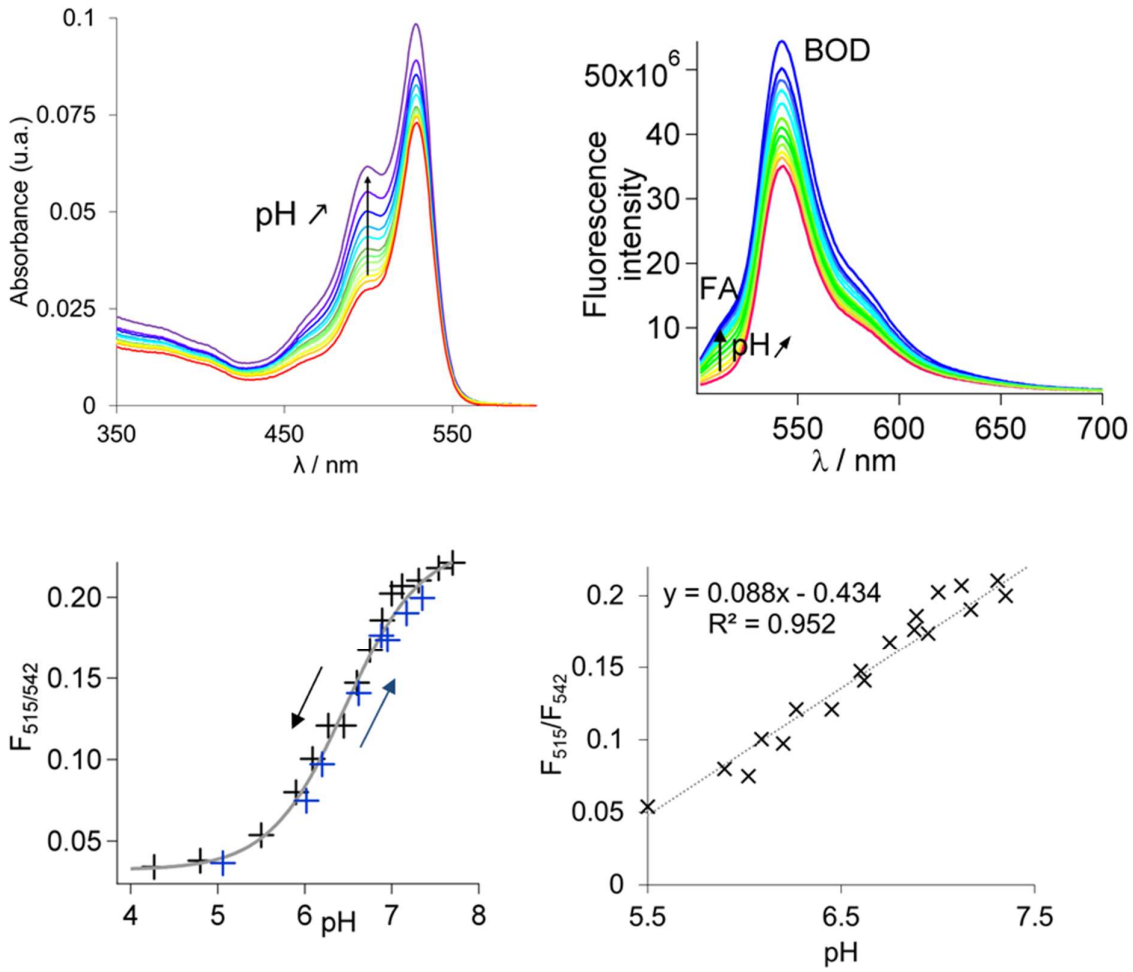

Figure S12. Spectra of **FNP2$_{BOD-FA}$** at various pH (λ_{exc} = 495 nm; phosphate/citrate buffers 10mM in 140mM NaCl; pH values: 7.70, 7.54, 7.31, 7.00, 6.89, 6.75, 6.60, 6.45, 6.27, 6.09, 5.90, 5.50, 4.80, 4.27). Top left: absorption. Top right: fluorescence emission (λ_{exc} = 495 nm. Bottom left: variation of the ratio of fluorescence intensity at 515 and 542 nm as a function of the pH (+) and fit using the Henderson-Hasselbach equation 2 with pK_a = 6.47 (—). Grey points correspond to a decrease in pH and blue ones to an increase. Bottom right: variation of the ratio of fluorescence intensity at 515 and 542 nm as a function of the pH (between pH = 5.5 and 7.5) and fit using a linear equation.

Excitation spectra of all FNP

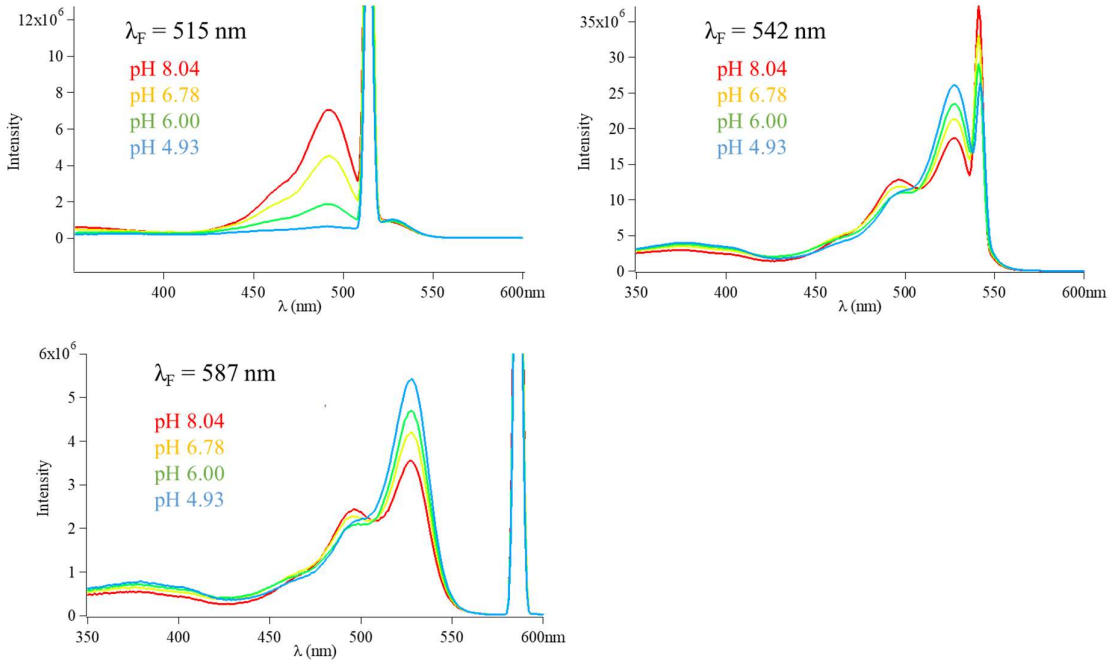

Figure S13 Excitation spectra of $FNP1_{BOD\text{-}FA}$ recorded at 3 different emission wavelengths (λ_F = 515, 542 or 587 nm) and at 4 different pH (8.04, 6.78, 6.00, 4.93).

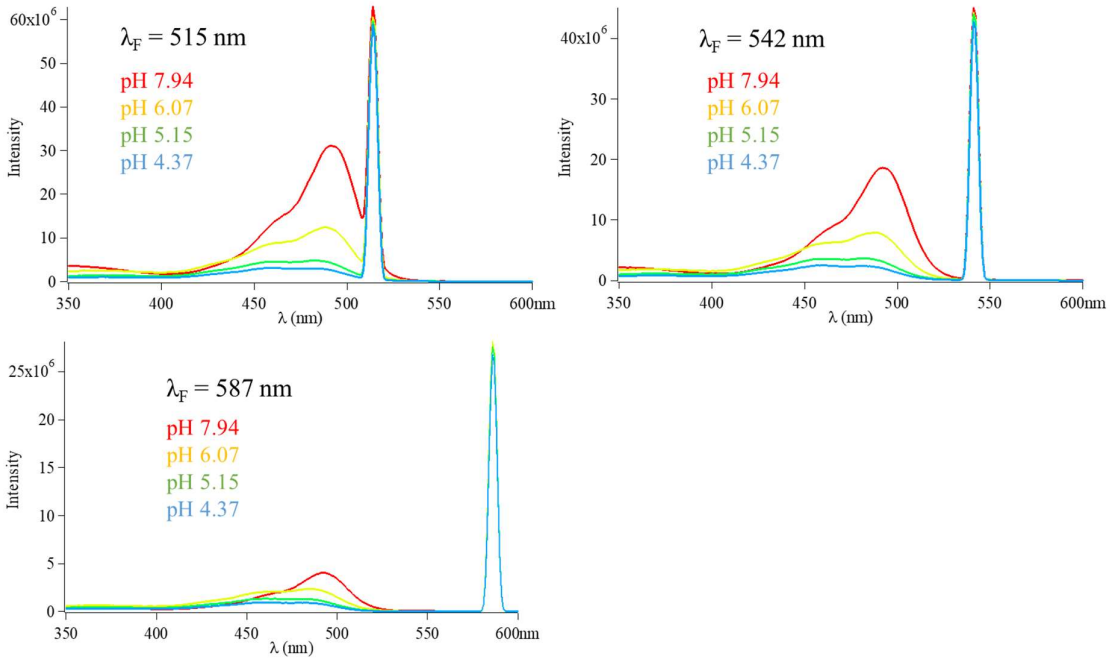

Figure S14 Excitation spectra of $FNP1_{FA}$ recorded at 3 different emission wavelengths (λ_F = 515, 542 or 587 nm) and at 4 different pH (7.94, 6.07, 5.15, 4.37).

Fluorescence decays

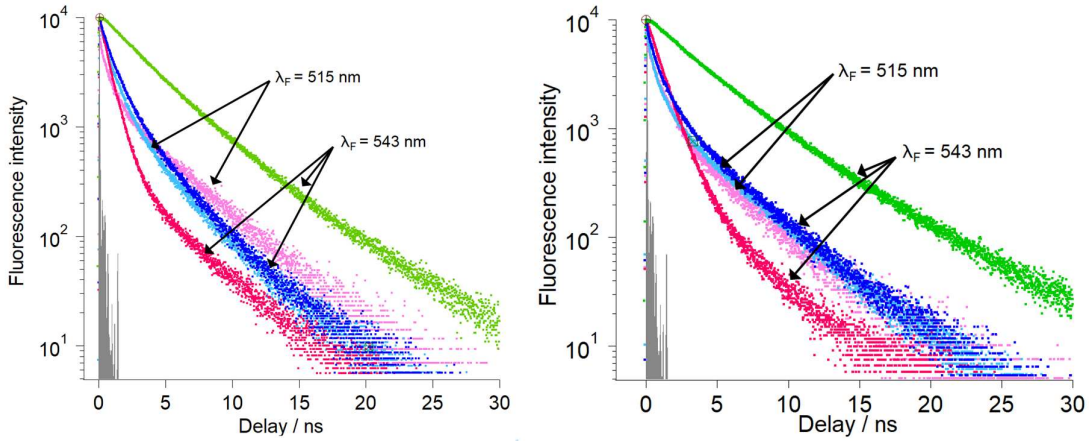

Figure S15. Fluorescence decays recorded in water at λ_F = 515 (lighter colors) and 543 nm (darker colors) (pH=7.8, λ_{ex} = 495 nm). Left: **FNP1$_{BOD}$** (green), **FNP1$_{FA}$** (blue) and **FNP1$_{BOD-FA}$** (pink). Right: **FNP2$_{BOD}$** (green), **FNP2$_{FA}$** (blue) and **FNP2$_{BOD-FA}$** (pink). Grey line is the instrument response function (IRF).

Multivariate curve resolution

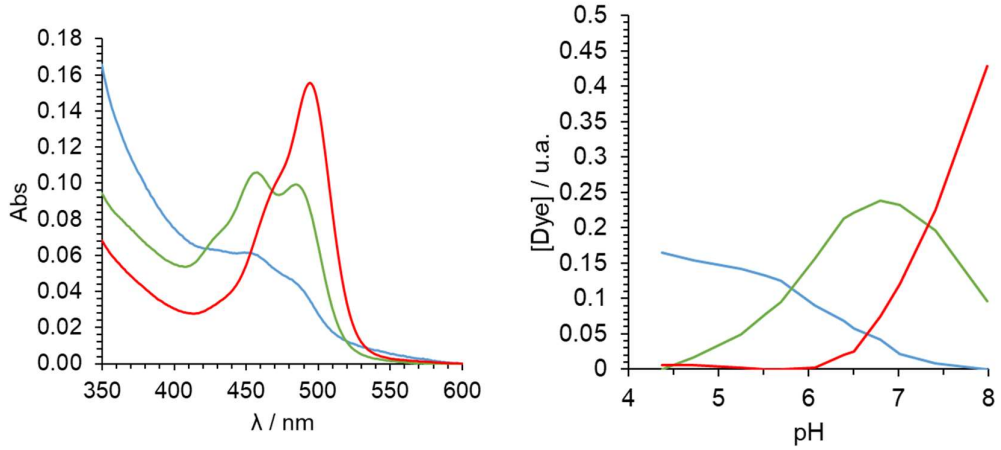

Figure S16. Left: spectral shape obtained from the multivariate curve resolution of the absorption spectra of **FNP1$_{FA}$** as a function of pH. The red spectrum corresponds to the one of the FA dianion, the green one to its anion and the blue to the neutral form. The increase in absorption at shorter wavelength is due to the scattering of light by the FNP. Right: distribution of the concentrations of the three species corresponding to the spectra on the left as a function of pH (same color code).

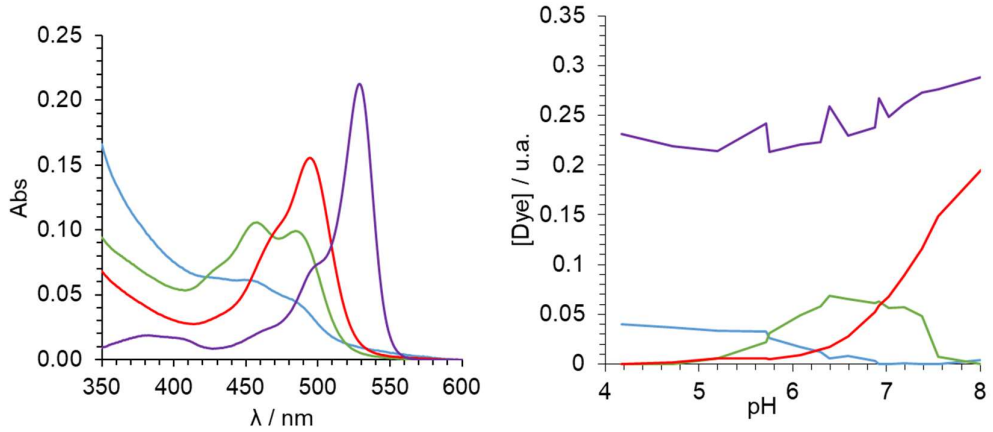

Figure S17. Left: spectral shape obtained from the multivariate curve resolution of the absorption spectra of **FNP1$_{BOD\text{-}FA}$** as a function of pH. The red spectrum corresponds to the one of the FA dianion, the green one to its anion and the blue to the neutral form and the purple one to the BODIPY. The increase in absorption at lower wavelength is due to the diffusion of light by the FNP. Right: distribution of the concentrations of the four species corresponding to the spectra on the left as a function of pH (same color code). The distribution for the FA components matches the one obtained with **FNP1$_{FA}$** while the contribution of the BODIPY shows a small variation.

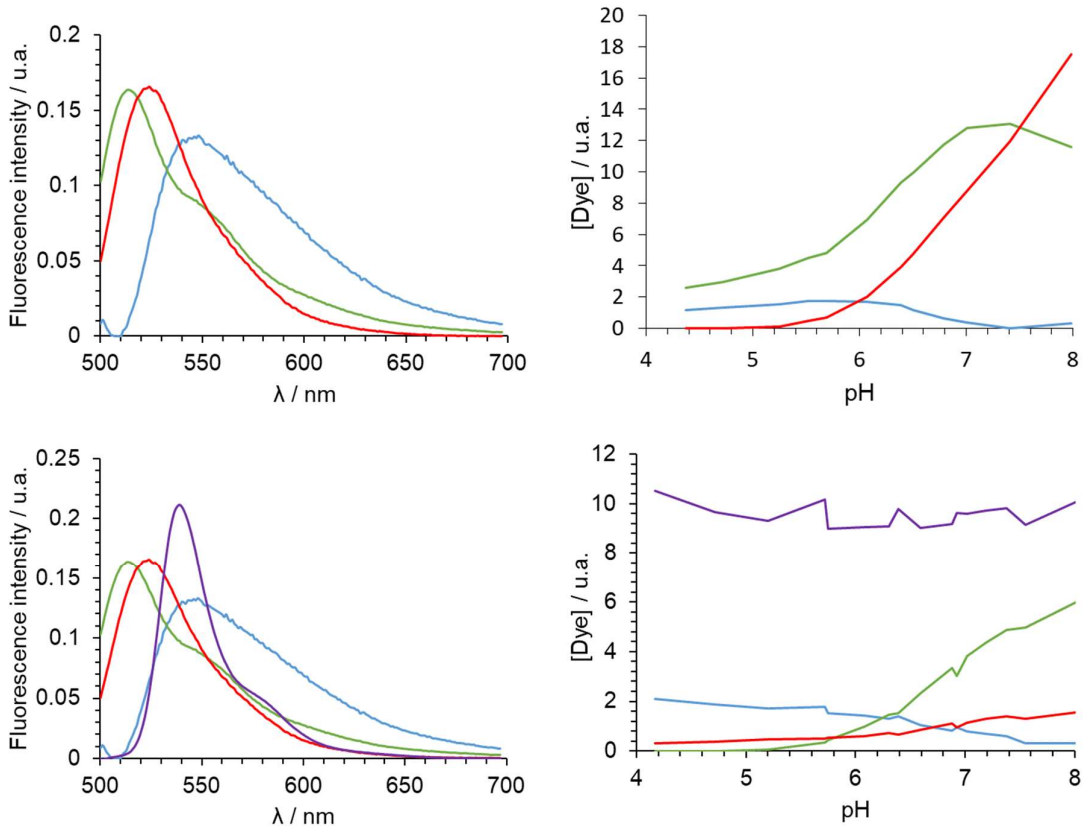

Figure S18. Top left: spectral shapes obtained from multivariate curve resolution of the emission spectra of **FNP1$_{FA}$** at different pH (from figure S9). The red spectrum matches the FA dianion, but the green and blue spectra do not correspond to known forms of the FA at different pH. Top right: distribution of the contributions of the three species corresponding to the spectra above as a function of pH (same color code). Bottom left: spectral shapes obtained from the principal component analysis of the emission spectra of **FNP1$_{BOD\text{-}FA}$** at different pH (from figure 2 left). The purple spectrum matches the BODIPY, the three other contributions are identical to the previous ones. Bottom right: distribution of the contributions of the four species corresponding to the spectra above as a function of pH (same color code). The contribution of the BODIPY shows small variation (5%) across the pH range studied.